
Implicit Contrastive Representation Learning with Guided Stop-gradient

Byeongchan Lee*

Gauss Labs
Seoul, Korea
byeongchan.lee@gausslabs.ai

Sehyun Lee*

KAIST
Daejeon, Korea
sehyun.lee@kaist.ac.kr

Abstract

In self-supervised representation learning, Siamese networks are a natural architecture for learning transformation-invariance by bringing representations of positive pairs closer together. But it is prone to collapse into a degenerate solution. To address the issue, in contrastive learning, a contrastive loss is used to prevent collapse by moving representations of negative pairs away from each other. But it is known that algorithms with negative sampling are not robust to a reduction in the number of negative samples. So, on the other hand, there are algorithms that do not use negative pairs. Many positive-only algorithms adopt asymmetric network architecture consisting of source and target encoders as a key factor in coping with collapse. By exploiting the asymmetric architecture, we introduce a methodology to implicitly incorporate the idea of contrastive learning. As its implementation, we present a novel method guided stop-gradient. We apply our method to benchmark algorithms SimSiam and BYOL and show that our method stabilizes training and boosts performance. We also show that the algorithms with our method work well with small batch sizes and do not collapse even when there is no predictor. The code is available at <https://github.com/bych-lee/gsg>.

1 Introduction

Representation learning has been a critical topic in machine learning. In visual representation learning, image representations containing high-level semantic information (e.g., visual concept) are learned for efficient training in downstream tasks. Because human annotation is labor-intensive and imperfect, learning representations without labels is getting more attention. In many cases, unsupervised or self-supervised learning (SSL) has surpassed its supervised counterpart.

In SSL [Jaiswal et al., 2020, Jing and Tian, 2020, Liu et al., 2021], there are roughly two branches of algorithms. One branch is a set of algorithms trained on pretext tasks with pseudo labels. Examples of the pretext tasks are predicting relative positions [Doersch et al., 2015], solving jigsaw puzzles [Noroozi and Favaro, 2016], colorization [Zhang et al., 2016], and identifying different rotations [Gidaris et al., 2018]. However, relying on a specific pretext task can restrict the generality of the learned representations. The other branch is a set of algorithms trained by maximizing the agreement of representations of randomly augmented views from the same image. Many algorithms in this branch adopt Siamese networks with two parallel encoders as their architecture. Siamese networks are natural architecture with a minimal inductive bias to learn transformation-invariant representations. However, naïve use of Siamese networks can result in collapse, i.e., a constant representation for all images.

To tackle the collapse problem, there have been four strategies. The first strategy is contrastive learning [Bachman et al., 2019, Ye et al., 2019, Chen et al., 2020a,b, He et al., 2020, Misra and Maaten,

*These authors contributed equally to this work.

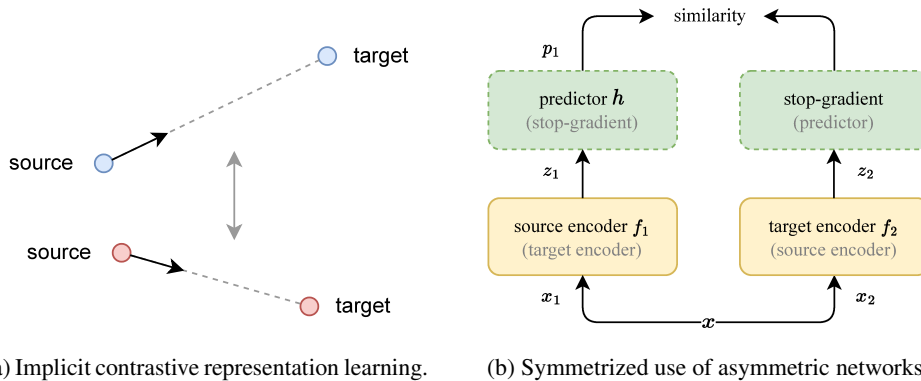


Figure 1: (a) Dots of the same color are representations of a positive pair. Without contrastive loss, it aims for a repelling effect by carefully determining which to make the source representation and which to make the target representation. (b) In SimSiam and BYOL, a given image x is randomly transformed into two views x_1 and x_2 . The views are processed by encoders f_1 and f_2 to have projections z_1 and z_2 . A predictor is applied on one side, and stop-gradient is applied on the other. Then, the similarity between the outputs from both sides is maximized. By using the predictor and stop-gradient alternately, a symmetric loss is constructed.

2020, Chen et al., 2021]. Contrastive learning uses positive pairs (views of the same image) and negative pairs (views from different images). Minimizing contrastive loss encourages representations of negative pairs to push each other while representations of positive pairs pull each other. The second strategy is to use clustering [Caron et al., 2018, Asano et al., 2019, Caron et al., 2019, 2020, Li et al., 2020]. It clusters the representations and then predicts the cluster assignment. Repeating this process keeps the cluster assignments consistent for positive pairs. The third strategy is to decorrelate between other variables of representations while maintaining the variance of each variable so that it does not get small [Bardes et al., 2021, Zbontar et al., 2021]. The fourth strategy is to break the symmetry of Siamese networks [Caron et al., 2020, Grill et al., 2020, He et al., 2020, Caron et al., 2021, Chen and He, 2021]. Many algorithms using this strategy make the representation from one encoder (called source encoder) follow the representation from the other encoder (called target encoder)².

In this paper, we introduce a methodology to do contrastive learning implicitly by leveraging asymmetric relation between the source and target encoders. For a given positive pair, one of its representations becomes the source representation (from the source encoder), and the other becomes the target representation (from the target encoder). The target representation attracts the source representation. By investigating how representations are located in the embedding space, we carefully determine which representation will be the source (or target) representation so that representations of negative pairs repel each other (Figure 1a). There is no explicit contrastive part in our loss, thus the name implicit contrastive representation learning. The main idea of the methodology can be expressed as follows: *Repel in the service of attracting*. We also present our guided stop-gradient method, an instance of the methodology. Our method can be applied to existing algorithms SimSiam [Chen and He, 2021] and BYOL [Grill et al., 2020]. We show that by applying our method, the performance of the original algorithms is boosted on various tasks and datasets.

The technical contributions of our work can be summarized as follows:

- We introduce a new methodology called implicit contrastive representation learning that exploits the asymmetry of network architecture for contrastive learning (Section 3 and 4).
- We present new algorithms by applying our method to benchmark algorithms SimSiam and BYOL and show performance improvements in various tasks and datasets (Section 5).
- We demonstrate through empirical studies that our idea can be used to improve training stability to help prevent collapse, which is a fundamental problem of SSL (Section 6).

²The source encoder is also called online, query, or student encoder, and the target encoder is also called key or teacher encoder in the literature depending on the context [Wang et al., 2022, Tarvainen and Valpola, 2017, Grill et al., 2020, He et al., 2020, Caron et al., 2021].

2 Related work

Siamese networks Siamese networks are symmetric in many respects. There are encoders of the same structure on both sides, and they share weights. The inputs to the two encoders have the same distribution, and the outputs are induced to be similar by the loss. On the one hand, this symmetric structure helps to learn transformation-invariance well, but on the other hand, all representations risk collapsing to a trivial solution. There have been several approaches to solving this collapse problem, and the approaches related to our work are contrastive learning and asymmetric learning. So, we introduce them in more detail below.

Contrastive learning Contrastive learning [Hadsell et al., 2006, Wang and Isola, 2020, Wu et al., 2018, Hjelm et al., 2018, Tian et al., 2020] can be characterized by its contrastive loss [Le-Khac et al., 2020, Chopra et al., 2005]. The basic idea is to design the loss so that representations of positive pairs pull together and representations of negative pairs push away. Through the loss, representations are formed where equilibrium is achieved between the pulling and pushing forces. Contrastive losses that have been used so far include noise contrastive estimation (NCE) loss [Gutmann and Hyvärinen, 2010], triplet loss [Schroff et al., 2015], lifted structured loss [Oh Song et al., 2016], multi-class N -pair loss [Sohn, 2016], InfoNCE loss [Oord et al., 2018], soft-nearest neighbors loss [Frosst et al., 2019], and normalized-temperature cross-entropy loss [Chen et al., 2020a]. All the losses mentioned above contain explicit terms in their formula that cause the negative pairs to repel each other. Under self-supervised learning scenarios, since we don't know the labels, a negative pair simply consists of views from different images. Then, in practice, there is a risk that the negative pair consists of views from images with the same label, and performance degradation occurs due to this sampling bias [Chuang et al., 2020]. In addition, contrastive learning algorithms are sensitive to changes in the number of negative samples, so performance deteriorates when the number of negative samples is small.

Asymmetric learning Another approach to avoid collapse is to break the symmetry of Siamese networks and introduce asymmetry [Wang et al., 2022]. Asymmetry can be imposed on many aspects, including data, network architectures, weights, loss, and training methods. In MoCo [He et al., 2020], the encoders do not simply share weights, and the weights of one encoder (key encoder) are a moving average of the weights of the other encoder (query encoder). This technique of slowly updating an encoder is called a momentum encoder. SwAV [Caron et al., 2020] and DINO [Caron et al., 2021] apply a multi-crop strategy when performing data augmentation to make the distribution of inputs into encoders different. Also, the loss applied to the outputs from the encoders is asymmetric. Furthermore, in DINO, stop-gradient is applied to the output of one encoder (teacher encoder) and not the other (student encoder). In SimSiam [Chen and He, 2021] and BYOL [Grill et al., 2020], an additional module called predictor is stacked on one encoder (source encoder), and stop-gradient is applied to the output from the other encoder (target encoder). Compared to SimSiam, in BYOL, the target encoder is a momentum encoder.

3 Main idea

In this section, we explain our motivation and intuition behind our method using an example.

Asymmetric architecture In SimSiam and BYOL, for a given image x , two views x_1 and x_2 are generated by random transformations. The views are fed to encoders f_1 and f_2 to yield projections z_1 and z_2 . An encoder is a backbone plus a projector³. Then, a predictor h is applied to one encoder (source encoder) to have a prediction, and stop-gradient⁴ is applied to the other encoder (target encoder). The algorithms maximize the similarity between the resulting prediction and projection. The difference between SimSiam and BYOL is in the weights of the encoders. In SimSiam, the source and target encoder share the weights. On the other hand, in BYOL, the target encoder is a momentum encoder. That is, the weights of the target encoder are an exponential moving average of the weights of the source encoder. Due to the existence of the predictor and stop-gradient (also momentum encoder in the case of BYOL), the algorithms have asymmetric architecture (Figure 1b).

³Ultimately, we use representations from the backbone, but it is common practice to compose the loss with projections from the projector, i.e., the encoder [Chen et al., 2020a].

⁴Applying stop-gradient to z means treating z as a constant. In actual implementation, z is detached from the computational graph to prevent the propagation of the gradient.

Symmetric loss Despite the asymmetry of the architecture, the losses in SimSiam and BYOL are symmetrized. After alternately applying a predictor and stop-gradient to the two encoders, the following loss is obtained by adding the resulting loss terms:

$$\mathcal{L} = \frac{1}{2}\mathcal{D}(p_1, \text{sg}(z_2)) + \frac{1}{2}\mathcal{D}(p_2, \text{sg}(z_1)), \quad (1)$$

where $\mathcal{D}(\cdot, \cdot)$ denotes negative cosine similarity, i.e., $\mathcal{D}(p, z) = -(p/\|p\|_2) \cdot (z/\|z\|_2)$, and $\text{sg}(\cdot)$ denotes the stop-gradient operator. The range of possible values for the loss is $[-1, 1]$. Minimizing the first term brings p_1 (closely related to z_1) closer to z_2 , and minimizing the second term brings p_2 (closely related to z_2) closer to z_1 . By minimizing the loss, we want to move z_1 in the direction of z_2 and z_2 in the direction of z_1 .

Guided stop-gradient The main idea of our guided stop-gradient method is to design an asymmetric loss to leverage the asymmetry of the architecture. In other words, we select one of the two loss terms in Equation (1) to help with training. However, it is known that randomly constructing an asymmetric loss is not beneficial [Chen and He, 2021]. To do this systematically, we consider two different images x_1 and x_2 simultaneously and let each other be a reference. When trying to bring the representations of one image closer, we give a directional guide on which representation to apply stop-gradient to by utilizing the geometric relationship with the representations of the other reference image.

Specifically, let z_{11} (p_{11}) and z_{12} (p_{12}) be projections (predictions) from the image x_1 , and z_{21} (p_{21}) and z_{22} (p_{22}) be projections (predictions) from the image x_2 . Then, the symmetrized loss for two images will be as follows (Figure 2a):

$$\mathcal{L} = \frac{1}{4}\mathcal{D}(p_{11}, \text{sg}(z_{12})) + \frac{1}{4}\mathcal{D}(p_{12}, \text{sg}(z_{11})) + \frac{1}{4}\mathcal{D}(p_{21}, \text{sg}(z_{22})) + \frac{1}{4}\mathcal{D}(p_{22}, \text{sg}(z_{21})). \quad (2)$$

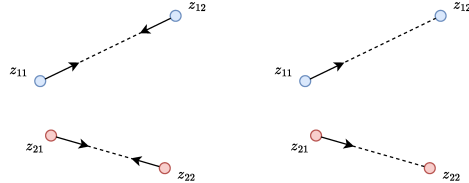
Now, we select one term from the first two terms (terms to maximize agreement between z_{11} and z_{12}) and another term from the remaining two terms (terms to maximize agreement between z_{21} and z_{22}). One view of the image x_1 and one view of the image x_2 form a negative pair. So we want the projections of the image x_1 and the projections of the image x_2 not to be close to each other. In the example of Figure 2, since z_{11} and z_{21} are closest, we apply a predictor⁵ to z_{11} and z_{21} and apply stop-gradient to z_{12} and z_{22} to try to separate the projections. Then, the resulting loss will be as follows (Figure 2b):

$$\mathcal{L} = \frac{1}{2}\mathcal{D}(p_{11}, \text{sg}(z_{12})) + \frac{1}{2}\mathcal{D}(p_{21}, \text{sg}(z_{22})). \quad (3)$$

Selecting loss terms is equivalent to determining which of the two projections of each image to apply stop-gradient. Since we do this in a guided way by observing how the projections are located, we call the method Guided Stop-Gradient (GSG). In this way, by continuously moving toward representations that are not close together, representations of negative pairs are induced to spread well in the long run.

Implicit contrastive representation learning In our loss, there is no explicit part where the projections of a negative pair repulse each other. However, the loss we designed implicitly does it. We aim for a contrastive effect by making good use of the fact that the source projections go after the target projections in an asymmetric network architecture. Therefore, SimSiam and BYOL with GSG can also be viewed as a mixture of contrastive learning and asymmetric learning.

⁵In the case of SimSiam and BYOL, the presence of a predictor can make the interpretation tricky because when we move two close points z and z' , we move them indirectly by moving $p = h(z)$ and $p' = h(z')$ through the predictor h . We assume that the predictor h has a good regularity as a function, that is, if $\|z - z'\|_2$ is small, $\|h(z) - h(z')\|_2$ is also small. So, by trying to separate p and p' , we separate z and z' . Note that in practice, the predictor h is usually an MLP with a few layers.



(a) Loss terms for two imgs. (b) Selected loss terms.

Figure 2: An example for two images. The dots represent four projections of the two images. The arrows represent the expected effect of the loss terms. We want dots of the same color to come close to each other. We select loss terms so that two closest dots with different colors will fall apart.

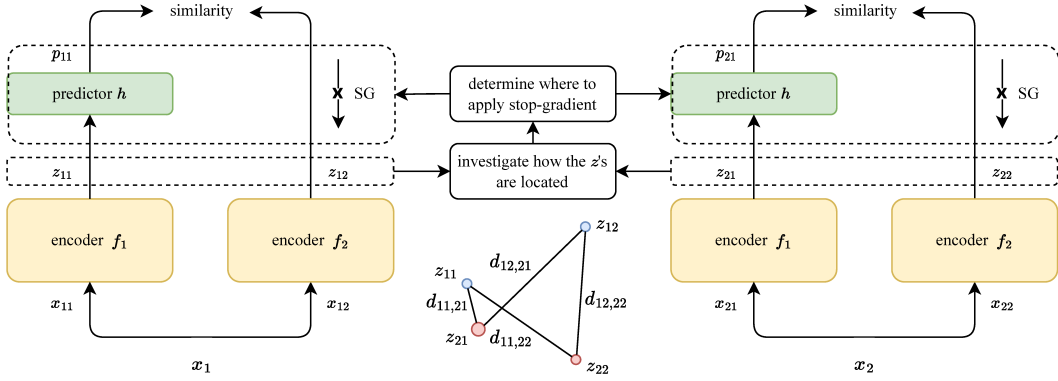


Figure 3: Overview of our guided stop-gradient method. (1) The encoders process two images x_1 , x_2 that are reference to each other. (2) Investigate the distances $d_{11,21}$, $d_{11,22}$, $d_{12,21}$, and $d_{12,22}$ between the projections of negative pairs. (3) Determine which side to apply stop-gradient and which to apply a predictor.

4 Method

In this section, we explain the specific application of GSG based on the main idea described above.

For a given batch of images for training, a batch of pairs of images is created by matching the images of the batch with the images of the shuffled batch one by one. Then, a pair of images in the resulting batch consists of two images, x_1 and x_2 . Note that since the images are paired within a given batch, the batch size is the same as the existing algorithm. By applying random augmentation, we generate views x_{11} and x_{12} from the image x_1 and views x_{21} and x_{22} from the image x_2 . The views are processed by an encoder f to yield projections z_{11} and z_{12} of the image x_1 and projections z_{21} and z_{22} of the image x_2 .

Let $d_{ij,kl}$ denote the Euclidean distance between projections z_{ij} and z_{kl} , i.e.,

$$d_{ij,kl} = \|z_{ij} - z_{kl}\|_2, \quad (4)$$

where $\|\cdot\|_2$ is l_2 -norm. We investigate distances $d_{11,21}$, $d_{11,22}$, $d_{12,21}$, and $d_{12,22}$. Note that there are four cases in total since we are looking at the distance between one of the two projections of x_1 and one of the two projections of x_2 . Now, we find the minimum m of the distances. That is,

$$m = \min\{d_{11,21}, d_{11,22}, d_{12,21}, d_{12,22}\}. \quad (5)$$

We apply a predictor to the two projections corresponding to the smallest of the four distances and stop-gradient to the remaining two projections. Depending on which distance is the smallest, the loss is as follows:

$$\mathcal{L} = \begin{cases} \frac{1}{2}\mathcal{D}(p_{11}, \text{sg}(z_{12})) + \frac{1}{2}\mathcal{D}(p_{21}, \text{sg}(z_{22})), & \text{if } m = d_{11,21} \\ \frac{1}{2}\mathcal{D}(p_{11}, \text{sg}(z_{12})) + \frac{1}{2}\mathcal{D}(p_{22}, \text{sg}(z_{21})), & \text{if } m = d_{11,22} \\ \frac{1}{2}\mathcal{D}(p_{12}, \text{sg}(z_{11})) + \frac{1}{2}\mathcal{D}(p_{21}, \text{sg}(z_{22})), & \text{if } m = d_{12,21} \\ \frac{1}{2}\mathcal{D}(p_{12}, \text{sg}(z_{11})) + \frac{1}{2}\mathcal{D}(p_{22}, \text{sg}(z_{21})), & \text{if } m = d_{12,22}. \end{cases} \quad (6)$$

For a better understanding, refer to Figure 3 and Appendix A. For simplicity, we present the overview and pseudocode for SimSiam with GSG, but they are analogous to BYOL with GSG.

5 Comparison

In this section, we compare SimSiam and BYOL with GSG to the original SimSiam and BYOL on various datasets and tasks. For a fair comparison, we use the same experimental setup for all four algorithms on each dataset and task. For example, all algorithms perform the same number of gradient updates and exploit the same number of images in each update. We implement the algorithms with Pytorch [Paszke et al., 2019] and run all the experiments on 8 NVIDIA A100 GPUs. Our algorithms take about two days for ImageNet pre-training and 12 hours for linear evaluation.

Table 1: Comparison of representation quality under standard evaluation protocols.

Algorithm	ImageNet		CIFAR-10	
	k -NN acc. (%)	Linear acc. (%)	k -NN acc. (%)	Linear acc. (%)
SimSiam	51.7±0.11	67.9±0.09	77.0±0.67	82.7±0.26
SimSiam w/ GSG	58.4±0.17	69.4±0.02	82.2±0.48	86.4±0.28
BYOL	56.5±0.16	69.9±0.02	85.4±0.24	88.0±0.09
BYOL w/ GSG	62.2±0.06	71.1±0.12	89.4±0.21	90.3±0.16

Table 2: Comparison in transfer learning for image recognition.

Algorithm	CIFAR-10	Aircraft	Caltech	Cars	DTD	Flowers	Food	Pets	SUN397	VOC2007
SimSiam	90.0	39.7	86.5	31.8	70.9	88.8	61.6	81.4	57.8	80.5
SimSiam w/ GSG	92.3	47.0	89.6	41.2	73.0	89.5	64.3	85.1	59.8	82.6
BYOL	91.0	42.5	88.9	39.3	71.7	89.1	64.0	85.3	60.4	82.2
BYOL w/ GSG	93.6	47.1	89.9	46.9	72.6	89.5	67.1	89.1	61.6	82.7

5.1 Pre-training

We first pre-train networks in an unsupervised manner. The trained networks will later be used in downstream tasks. We use ImageNet [Deng et al., 2009] and CIFAR-10 [Krizhevsky et al., 2009] as benchmark datasets. Refer to Appendix B for data augmentation details.

For ImageNet, we use the ResNet-50 backbone [He et al., 2016], a three-layered MLP projector, and a two-layered MLP predictor. We use a batch size of 512 and train the network for 100 epochs. We use the SGD optimizer with momentum of 0.9, learning rate of 0.1, and weight decay rate of 0.0001. We use a cosine decay schedule [Chen et al., 2020a, Loshchilov and Hutter, 2016] for the learning rate.

For CIFAR-10, we use a CIFAR variant of the ResNet-18 backbone, a two-layered MLP projector, and a two-layered MLP predictor. We use a batch size of 512 and train the network for 200 epochs. We use the SGD optimizer with momentum of 0.9, learning rate of 0.06, and weight decay rate of 0.0005. We do not use a learning rate schedule since no scaling shows better training stability. Refer to Appendix C for other implementation details.

After pre-training, we obtain representations of the images with the trained backbone and then evaluate their quality. We use both k -nearest neighbors [Wu et al., 2018] and linear evaluation, which are standard evaluation protocols.

k -nearest neighbors For a given test set image, we find its representation and obtain k training set images with the closest representation. Then, we determine the predicted label of the image by majority voting of the labels of the k images. We set $k = 200$ for ImageNet and $k = 1$ for CIFAR-10.

Linear evaluation We freeze the trained backbone, attach a linear classifier to the backbone, fit the classifier on the training set in a supervised manner for 90 epochs, and test the classifier on the test set. For ImageNet, we use a batch size of 4096 and the LARS optimizer [You et al., 2017], which can work well with a large batch size. For CIFAR-10, we use a batch size of 256 and the SGD optimizer with momentum of 0.9, learning rate of 30, and a cosine decay schedule. We report top-1 accuracy for all cases.

Results Table 1 shows that applying GSG consistently increases the performance. We report error bars (mean \pm standard deviation) by running each algorithm three times independently and show that our method improves the performance reliably. The performance gain is obtained by keeping all other experimental setups the same and changing only the stop-gradient application method. This suggests that there is room for improvement in the symmetrized use of asymmetric networks in the existing algorithms.

Table 3: Comparison in transfer learning for object detection and semantic segmentation.

Algorithm	VOC detection			COCO detection			Semantic segmentation	
	AP ₅₀	AP	AP ₇₅	AP ₅₀	AP	AP ₇₅	Mean IoU (%)	Pixel acc. (%)
SimSiam	77.0	48.8	52.2	50.7	31.2	32.8	0.2626	65.63
SimSiam w/ GSG	79.8	51.2	55.1	53.2	33.4	35.6	0.3345	76.57
BYOL	79.2	50.3	54.5	52.0	32.5	34.5	0.2615	62.79
BYOL w/ GSG	80.5	52.0	56.4	53.7	33.8	36.1	0.2938	74.78

Table 4: Comparison between explicit and implicit contrastive learning algorithms.

Methodology	Algorithm	$b = 1024$	$b = 512$	$b = 256$
Explicit contrastive	End-to-end [He et al., 2020]	57.3	56.3	54.9
	InstDisc [Wu et al., 2018]	54.1	52.0	50.0
	MoCo [He et al., 2020]	57.5	56.4	54.7
	SimCLR [Chen et al., 2020a]	62.8	60.7	57.5
Implicit contrastive	SimSiam w/ GSG	70.1	69.4	69.9
	BYOL w/ GSG	71.9	71.0	71.6

5.2 Transfer learning

An essential goal of representation learning is to obtain a pre-trained backbone that can be transferred to various downstream tasks. To evaluate whether our pre-trained backbones are transferable, we consider image recognition, object detection, and semantic segmentation tasks. We use the ResNet-50 backbones pre-trained on ImageNet. We follow the experimental setup in [Ericsson et al., 2021]. More implementation details can be found in Appendix D.

Image recognition We carry out image recognition tasks on different datasets. For datasets, we adopt widely used benchmark datasets in transfer learning such as CIFAR-10, Aircraft [Maji et al., 2013], Caltech [Fei-Fei et al., 2004], Cars [Krause et al., 2013], DTD [Cimpoi et al., 2014], Flowers [Nilsback and Zisserman, 2008], Food [Bossard et al., 2014], Pets [Parkhi et al., 2012], SUN397 [Xiao et al., 2010], and VOC2007 [Everingham et al., 2010]. These datasets vary in terms of the amount of data or the number of classes. We report the average precision AP at 11 recall levels $\{0, 0.1, \dots, 1\}$ on VOC2007, mean per-class accuracy on Aircraft, Pets, Caltech, and Flowers, and top-1 accuracy on the rest of the datasets. For the evaluation protocol, we perform the linear evaluation.

Object detection We perform object detection tasks on Pascal-VOC [Everingham et al., 2010] and MS-COCO [Lin et al., 2014]. We use VOC2007 trainval as the training set and VOC2007 test as the test set. We report AP₅₀, AP, and AP₇₅. AP₅₀ and AP₇₅ are average precision with intersection over union (IoU) threshold 0.5 and 0.75, respectively. We freeze the pre-trained backbone except for the last residual block. We use a Feature Pyramid Network [Lin et al., 2017] to extract representations, and a Faster R-CNN [Ren et al., 2015] to predict. We do the experiments on the Detectron2 platform [Wu et al., 2019].

Semantic segmentation We conduct semantic segmentation tasks on MIT ADE20K [Zhou et al., 2019]. We use ResNet-50 as the encoder and use UPerNet [Xiao et al., 2018] (the implementation in the CSAIL semantic segmentation framework [Zhou et al., 2018, 2017]) as the decoder. It is based on Feature Pyramid Network and Pyramid Pooling Module [Zhao et al., 2017]. We train for 30 epochs and test on the validation set. We report mean IoU and pixel accuracy. For the predicted results of each algorithm, refer to Appendix F.

Results Table 2 and 3 show that applying GSG increases the performance consistently. We can conclude that the pre-trained backbones are transferable to different tasks, and our method helps to get better quality representations.

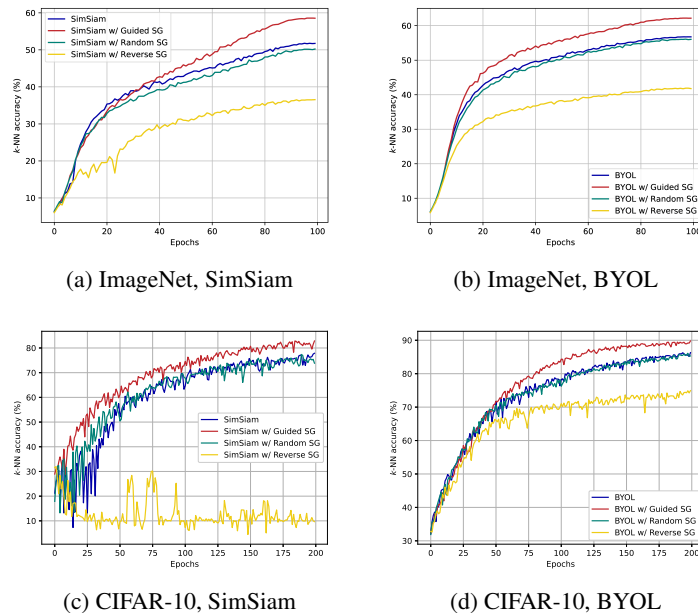


Figure 4: Importance of guiding. Depending on how stop-gradient is used, performance is significantly different. It shows the best performance when used along with GSG.

5.3 The number of negative samples

It is known that the performance of contrastive learning algorithms is vulnerable to reducing the number of negative samples [Tian et al., 2020, Wu et al., 2018, He et al., 2020, Chen et al., 2020a]. In this respect, we compare our algorithms to benchmark contrastive learning algorithms (all with the ResNet-50 backbone). Table 4 reports linear evaluation accuracy on ImageNet (the performance of the benchmark algorithms is from [He et al., 2020] and [Chen et al., 2020a]). End-to-end, SimCLR, and our algorithms use samples in the batch as negative samples, so for these algorithms, b in the table denotes the batch size. InstDisc and MoCo maintain a separate memory bank or dictionary, so for these algorithms, b in the table denotes the number of negative samples from the memory bank or dictionary. The table shows that our algorithms work well with small batch sizes.

6 Empirical study

In this section, we broaden our understanding of stop-gradient, predictor, and momentum encoder, which are components of SimSiam and BYOL by comparing variants of the algorithms.

6.1 Importance of guiding

We demonstrate that it is crucial to apply stop-gradient in a guided way by changing how stop-gradient is used. We compare our GSG with what we name random stop-gradient and reverse stop-gradient. In random stop-gradient, stop-gradient is randomly applied to one of the two encoders, and a predictor is applied to the other. That is, we randomly select one of the four equations in Equation (6). On the other hand, in reverse stop-gradient, stop-gradient is applied opposite to the intuition in GSG. In other words, we select the remaining loss terms other than the selected loss terms when GSG is used. In Equation (2), two loss terms will be selected to form the loss as follows:

$$\mathcal{L} = \frac{1}{2}\mathcal{D}(p_{12}, \text{sg}(z_{11})) + \frac{1}{2}\mathcal{D}(p_{22}, \text{sg}(z_{21})). \quad (7)$$

Therefore, the random stop-gradient is a baseline where stop-gradient is naïvely applied, and the reverse stop-gradient is the worst-case scenario according to our intuition.

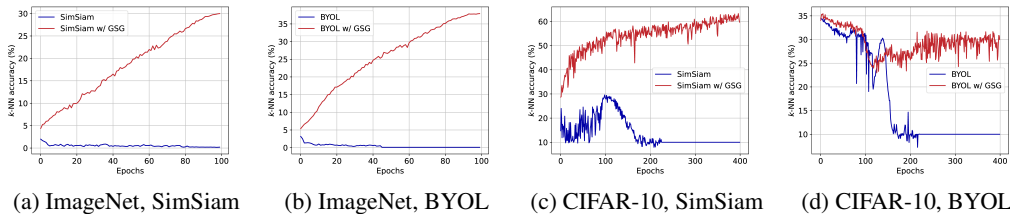


Figure 5: Preventing collapse. Unlike existing algorithms, algorithms to which GSG is applied do not collapse even when the predictor is removed.

Figure 4 shows the results of applying GSG, random stop-gradient, and reverse stop-gradient along with the existing algorithm for SimSiam and BYOL. We observe the k -NN accuracy at each epoch while training on ImageNet and CIFAR-10. First of all, in all cases, it can be seen that the algorithm applying our GSG outperforms algorithms using other methods. In addition, it can be seen that the performance of the existing algorithm and the algorithm to which random stop-gradient is applied are similar. When applying random stop-gradient, the number of loss terms is doubled, and half of them are randomly selected, so there is expected to be no significant difference from the existing algorithm. In the case of reverse stop-gradient, the performance drops significantly. This highlights the importance of using stop-gradient in a guided manner.

If we look at the case of CIFAR-10 (Figure 4c and Figure 4d), which has relatively much smaller data and is more challenging to train stably, we can obtain some more interesting results. First, when reverse stop-gradient is applied to SimSiam, it collapses, and the accuracy converges to 10%, which is the chance-level accuracy of CIFAR-10. However, this was not the case for BYOL. This implies that the momentum encoder can help prevent collapse. Note that SimSiam and BYOL are identical in our experimental setup, except that BYOL has a momentum encoder. In addition, in the case of the existing SimSiam and SimSiam with random stop-gradient, the fluctuation of the accuracy at the beginning of training is severe. However, it is relatively less in the case of SimSiam with GSG. This suggests that GSG can help the stability of training.

6.2 Preventing collapse

One of the expected effects of GSG is to prevent collapse by implicitly repelling each other away from negative pairs. It is known that SimSiam and BYOL collapse without a predictor [Chen and He, 2021, Grill et al., 2020]. Then, a natural question is whether SimSiam and BYOL will not collapse even if the predictor is removed when GSG is applied. Figure 5 reports the performance when the predictor is removed. In the case of CIFAR-10, we run up to 400 epochs to confirm complete collapse.

First, the existing algorithms collapse as expected, and the accuracy converges to the chance-level accuracy (0.1% for ImageNet and 10% for CIFAR-10). Interestingly, however, our algorithms do not collapse. This shows that GSG contributes to training stability, which is our method’s intrinsic advantage. Nevertheless, the final accuracy is higher when there is a predictor. This indicates that the predictor in SimSiam and BYOL contributes to performance improvement.

7 Conclusion

We have proposed implicit contrastive representation learning for visual SSL. In this methodology, while representations of positive pairs attract each other, representations of negative pairs are promoted to repel each other. It exploits the asymmetry of network architectures with source and target encoders without contrastive loss. We have instantiated the methodology and presented our guided stop-gradient method, which can be applied to existing SSL algorithms such as SimSiam and BYOL. We have shown that our algorithms consistently perform better than the benchmark asymmetric learning algorithms for various tasks and datasets. We have also shown that our algorithms are more robust to reducing the number of negative samples than the benchmark contrastive learning algorithms. Our empirical study has shown that our method contributes to training stability. We

hope our work leads the community to better leverage the asymmetry between source and target encoders and enjoy the advantages of both contrastive learning and asymmetric learning.

References

- Yuki Markus Asano, Christian Rupprecht, and Andrea Vedaldi. Self-labelling via simultaneous clustering and representation learning. *arXiv preprint arXiv:1911.05371*, 2019.
- Philip Bachman, R Devon Hjelm, and William Buchwalter. Learning representations by maximizing mutual information across views. *Advances in neural information processing systems*, 32, 2019.
- Adrien Bardes, Jean Ponce, and Yann LeCun. Vicreg: Variance-invariance-covariance regularization for self-supervised learning. *arXiv preprint arXiv:2105.04906*, 2021.
- Lukas Bossard, Matthieu Guillaumin, and Luc Van Gool. Food-101—mining discriminative components with random forests. In *Computer Vision—ECCV 2014: 13th European Conference, Zurich, Switzerland, September 6–12, 2014, Proceedings, Part VI 13*, pages 446–461. Springer, 2014.
- Mathilde Caron, Piotr Bojanowski, Armand Joulin, and Matthijs Douze. Deep clustering for unsupervised learning of visual features. In *Proceedings of the European conference on computer vision (ECCV)*, pages 132–149, 2018.
- Mathilde Caron, Piotr Bojanowski, Julien Mairal, and Armand Joulin. Unsupervised pre-training of image features on non-curated data. In *Proceedings of the IEEE/CVF International Conference on Computer Vision*, pages 2959–2968, 2019.
- Mathilde Caron, Ishan Misra, Julien Mairal, Priya Goyal, Piotr Bojanowski, and Armand Joulin. Unsupervised learning of visual features by contrasting cluster assignments. *Advances in Neural Information Processing Systems*, 33:9912–9924, 2020.
- Mathilde Caron, Hugo Touvron, Ishan Misra, Hervé Jégou, Julien Mairal, Piotr Bojanowski, and Armand Joulin. Emerging properties in self-supervised vision transformers. In *Proceedings of the IEEE/CVF International Conference on Computer Vision*, pages 9650–9660, 2021.
- Ting Chen, Simon Kornblith, Mohammad Norouzi, and Geoffrey Hinton. A simple framework for contrastive learning of visual representations. In *International conference on machine learning*, pages 1597–1607. PMLR, 2020a.
- Xinlei Chen and Kaiming He. Exploring simple siamese representation learning. In *Proceedings of the IEEE/CVF Conference on Computer Vision and Pattern Recognition*, pages 15750–15758, 2021.
- Xinlei Chen, Haoqi Fan, Ross Girshick, and Kaiming He. Improved baselines with momentum contrastive learning. *arXiv preprint arXiv:2003.04297*, 2020b.
- Xinlei Chen, Saining Xie, and Kaiming He. An empirical study of training self-supervised vision transformers. In *Proceedings of the IEEE/CVF International Conference on Computer Vision*, pages 9640–9649, 2021.
- Sumit Chopra, Raia Hadsell, and Yann LeCun. Learning a similarity metric discriminatively, with application to face verification. In *2005 IEEE Computer Society Conference on Computer Vision and Pattern Recognition (CVPR’05)*, volume 1, pages 539–546. IEEE, 2005.
- Ching-Yao Chuang, Joshua Robinson, Yen-Chen Lin, Antonio Torralba, and Stefanie Jegelka. De-biased contrastive learning. *Advances in neural information processing systems*, 33:8765–8775, 2020.
- Mircea Cimpoi, Subhansu Maji, Iasonas Kokkinos, Sammy Mohamed, and Andrea Vedaldi. Describing textures in the wild. In *Proceedings of the IEEE conference on computer vision and pattern recognition*, pages 3606–3613, 2014.
- Jia Deng, Wei Dong, Richard Socher, Li-Jia Li, Kai Li, and Li Fei-Fei. Imagenet: A large-scale hierarchical image database. In *2009 IEEE conference on computer vision and pattern recognition*, pages 248–255. Ieee, 2009.

- Carl Doersch, Abhinav Gupta, and Alexei A Efros. Unsupervised visual representation learning by context prediction. In *Proceedings of the IEEE international conference on computer vision*, pages 1422–1430, 2015.
- Linus Ericsson, Henry Gouk, and Timothy M Hospedales. How well do self-supervised models transfer? In *Proceedings of the IEEE/CVF Conference on Computer Vision and Pattern Recognition*, pages 5414–5423, 2021.
- Mark Everingham, Luc Van Gool, Christopher KI Williams, John Winn, and Andrew Zisserman. The pascal visual object classes (voc) challenge. *International journal of computer vision*, 88(2): 303–338, 2010.
- Li Fei-Fei, Rob Fergus, and Pietro Perona. Learning generative visual models from few training examples: An incremental bayesian approach tested on 101 object categories. In *2004 conference on computer vision and pattern recognition workshop*, pages 178–178. IEEE, 2004.
- Nicholas Frosst, Nicolas Papernot, and Geoffrey Hinton. Analyzing and improving representations with the soft nearest neighbor loss. In *International conference on machine learning*, pages 2012–2020. PMLR, 2019.
- Spyros Gidaris, Praveer Singh, and Nikos Komodakis. Unsupervised representation learning by predicting image rotations. *arXiv preprint arXiv:1803.07728*, 2018.
- Jean-Bastien Grill, Florian Strub, Florent Altché, Corentin Tallec, Pierre Richemond, Elena Buchatskaya, Carl Doersch, Bernardo Avila Pires, Zhaohan Guo, Mohammad Gheshlaghi Azar, et al. Bootstrap your own latent—a new approach to self-supervised learning. *Advances in neural information processing systems*, 33:21271–21284, 2020.
- Michael Gutmann and Aapo Hyvärinen. Noise-contrastive estimation: A new estimation principle for unnormalized statistical models. In *Proceedings of the thirteenth international conference on artificial intelligence and statistics*, pages 297–304. JMLR Workshop and Conference Proceedings, 2010.
- Raia Hadsell, Sumit Chopra, and Yann LeCun. Dimensionality reduction by learning an invariant mapping. In *2006 IEEE Computer Society Conference on Computer Vision and Pattern Recognition (CVPR’06)*, volume 2, pages 1735–1742. IEEE, 2006.
- Kaiming He, Xiangyu Zhang, Shaoqing Ren, and Jian Sun. Deep residual learning for image recognition. In *Proceedings of the IEEE conference on computer vision and pattern recognition*, pages 770–778, 2016.
- Kaiming He, Haoqi Fan, Yuxin Wu, Saining Xie, and Ross Girshick. Momentum contrast for unsupervised visual representation learning. In *Proceedings of the IEEE/CVF conference on computer vision and pattern recognition*, pages 9729–9738, 2020.
- R Devon Hjelm, Alex Fedorov, Samuel Lavoie-Marchildon, Karan Grewal, Phil Bachman, Adam Trischler, and Yoshua Bengio. Learning deep representations by mutual information estimation and maximization. *arXiv preprint arXiv:1808.06670*, 2018.
- Ashish Jaiswal, Ashwin Ramesh Babu, Mohammad Zaki Zadeh, Debapriya Banerjee, and Fillia Makedon. A survey on contrastive self-supervised learning. *Technologies*, 9(1):2, 2020.
- Longlong Jing and Yingli Tian. Self-supervised visual feature learning with deep neural networks: A survey. *IEEE transactions on pattern analysis and machine intelligence*, 43(11):4037–4058, 2020.
- Jonathan Krause, Jia Deng, Michael Stark, and Li Fei-Fei. Collecting a large-scale dataset of fine-grained cars. 2013.
- Alex Krizhevsky, Geoffrey Hinton, et al. Learning multiple layers of features from tiny images. 2009.
- Phuc H Le-Khac, Graham Healy, and Alan F Smeaton. Contrastive representation learning: A framework and review. *IEEE Access*, 8:193907–193934, 2020.

- Junnan Li, Pan Zhou, Caiming Xiong, and Steven CH Hoi. Prototypical contrastive learning of unsupervised representations. *arXiv preprint arXiv:2005.04966*, 2020.
- Tsung-Yi Lin, Michael Maire, Serge Belongie, James Hays, Pietro Perona, Deva Ramanan, Piotr Dollár, and C Lawrence Zitnick. Microsoft coco: Common objects in context. In *Computer Vision—ECCV 2014: 13th European Conference, Zurich, Switzerland, September 6–12, 2014, Proceedings, Part V 13*, pages 740–755. Springer, 2014.
- Tsung-Yi Lin, Piotr Dollár, Ross Girshick, Kaiming He, Bharath Hariharan, and Serge Belongie. Feature pyramid networks for object detection. In *Proceedings of the IEEE conference on computer vision and pattern recognition*, pages 2117–2125, 2017.
- Xiao Liu, Fanjin Zhang, Zhenyu Hou, Li Mian, Zhaoyu Wang, Jing Zhang, and Jie Tang. Self-supervised learning: Generative or contrastive. *IEEE Transactions on Knowledge and Data Engineering*, 2021.
- Ilya Loshchilov and Frank Hutter. Sgdr: Stochastic gradient descent with warm restarts. *arXiv preprint arXiv:1608.03983*, 2016.
- Subhansu Maji, Esa Rahtu, Juho Kannala, Matthew Blaschko, and Andrea Vedaldi. Fine-grained visual classification of aircraft. *arXiv preprint arXiv:1306.5151*, 2013.
- Ishan Misra and Laurens van der Maaten. Self-supervised learning of pretext-invariant representations. In *Proceedings of the IEEE/CVF Conference on Computer Vision and Pattern Recognition*, pages 6707–6717, 2020.
- Maria-Elena Nilsback and Andrew Zisserman. Automated flower classification over a large number of classes. In *2008 Sixth Indian Conference on Computer Vision, Graphics & Image Processing*, pages 722–729. IEEE, 2008.
- Mehdi Noroozi and Paolo Favaro. Unsupervised learning of visual representations by solving jigsaw puzzles. In *European conference on computer vision*, pages 69–84. Springer, 2016.
- Hyun Oh Song, Yu Xiang, Stefanie Jegelka, and Silvio Savarese. Deep metric learning via lifted structured feature embedding. In *Proceedings of the IEEE conference on computer vision and pattern recognition*, pages 4004–4012, 2016.
- Aaron van den Oord, Yazhe Li, and Oriol Vinyals. Representation learning with contrastive predictive coding. *arXiv preprint arXiv:1807.03748*, 2018.
- Omkar M Parkhi, Andrea Vedaldi, Andrew Zisserman, and CV Jawahar. Cats and dogs. In *2012 IEEE conference on computer vision and pattern recognition*, pages 3498–3505. IEEE, 2012.
- Adam Paszke, Sam Gross, Francisco Massa, Adam Lerer, James Bradbury, Gregory Chanan, Trevor Killeen, Zeming Lin, Natalia Gimelshein, Luca Antiga, et al. Pytorch: An imperative style, high-performance deep learning library. *Advances in neural information processing systems*, 32, 2019.
- Shaoqing Ren, Kaiming He, Ross Girshick, and Jian Sun. Faster r-cnn: Towards real-time object detection with region proposal networks. *Advances in neural information processing systems*, 28, 2015.
- Florian Schroff, Dmitry Kalenichenko, and James Philbin. Facenet: A unified embedding for face recognition and clustering. In *Proceedings of the IEEE conference on computer vision and pattern recognition*, pages 815–823, 2015.
- Kihyuk Sohn. Improved deep metric learning with multi-class n-pair loss objective. *Advances in neural information processing systems*, 29, 2016.
- Antti Tarvainen and Harri Valpola. Mean teachers are better role models: Weight-averaged consistency targets improve semi-supervised deep learning results. *Advances in neural information processing systems*, 30, 2017.
- Yonglong Tian, Dilip Krishnan, and Phillip Isola. Contrastive multiview coding. In *European conference on computer vision*, pages 776–794. Springer, 2020.

- Tongzhou Wang and Phillip Isola. Understanding contrastive representation learning through alignment and uniformity on the hypersphere. In *International Conference on Machine Learning*, pages 9929–9939. PMLR, 2020.
- Xiao Wang, Haoqi Fan, Yuandong Tian, Daisuke Kihara, and Xinlei Chen. On the importance of asymmetry for siamese representation learning. In *Proceedings of the IEEE/CVF Conference on Computer Vision and Pattern Recognition*, pages 16570–16579, 2022.
- Yuxin Wu, Alexander Kirillov, Francisco Massa, Wan-Yen Lo, and Ross Girshick. Detectron2. <https://github.com/facebookresearch/detectron2>, 2019.
- Zhirong Wu, Yuanjun Xiong, Stella X Yu, and Dahua Lin. Unsupervised feature learning via non-parametric instance discrimination. In *Proceedings of the IEEE conference on computer vision and pattern recognition*, pages 3733–3742, 2018.
- Jianxiong Xiao, James Hays, Krista A Ehinger, Aude Oliva, and Antonio Torralba. Sun database: Large-scale scene recognition from abbey to zoo. In *2010 IEEE computer society conference on computer vision and pattern recognition*, pages 3485–3492. IEEE, 2010.
- Tete Xiao, Yingcheng Liu, Bolei Zhou, Yuning Jiang, and Jian Sun. Unified perceptual parsing for scene understanding. In *Proceedings of the European conference on computer vision (ECCV)*, pages 418–434, 2018.
- Mang Ye, Xu Zhang, Pong C Yuen, and Shih-Fu Chang. Unsupervised embedding learning via invariant and spreading instance feature. In *Proceedings of the IEEE/CVF Conference on Computer Vision and Pattern Recognition*, pages 6210–6219, 2019.
- Yang You, Igor Gitman, and Boris Ginsburg. Large batch training of convolutional networks. *arXiv preprint arXiv:1708.03888*, 2017.
- Jure Zbontar, Li Jing, Ishan Misra, Yann LeCun, and Stéphane Deny. Barlow twins: Self-supervised learning via redundancy reduction. In *International Conference on Machine Learning*, pages 12310–12320. PMLR, 2021.
- Richard Zhang, Phillip Isola, and Alexei A Efros. Colorful image colorization. In *European conference on computer vision*, pages 649–666. Springer, 2016.
- Hengshuang Zhao, Jianping Shi, Xiaojuan Qi, Xiaogang Wang, and Jiaya Jia. Pyramid scene parsing network. In *Proceedings of the IEEE conference on computer vision and pattern recognition*, pages 2881–2890, 2017.
- Bolei Zhou, Hang Zhao, Xavier Puig, Sanja Fidler, Adela Barriuso, and Antonio Torralba. Scene parsing through ade20k dataset. In *Proceedings of the IEEE Conference on Computer Vision and Pattern Recognition*, 2017.
- Bolei Zhou, Hang Zhao, Xavier Puig, Tete Xiao, Sanja Fidler, Adela Barriuso, and Antonio Torralba. Semantic understanding of scenes through the ade20k dataset. *International Journal on Computer Vision*, 2018.
- Bolei Zhou, Hang Zhao, Xavier Puig, Tete Xiao, Sanja Fidler, Adela Barriuso, and Antonio Torralba. Semantic understanding of scenes through the ade20k dataset. *International Journal of Computer Vision*, 127:302–321, 2019.

Implicit Contrastive Representation Learning with Guided Stop-gradient - Appendix

Byeongchan Lee*
Gauss Labs
Seoul, Korea
byeongchan.lee@gausslabs.ai

Sehyun Lee*
KAIST
Daejeon, Korea
sehyun.lee@kaist.ac.kr

A Algorithm

We present a PyTorch-style pseudocode for SimSiam with GSG. It can be written analogously for BYOL with GSG. The pseudocode can be vectorized more, but we offer it in its current form for a better understanding.

Algorithm 1 SimSiam with GSG

```
# pytorch style pseudocode

for batch in loader:
    loss = []
    for x1, x2 in zip(batch, shuffle(batch)):
        x11, x12 = aug(x1), aug(x1) # views
        x21, x22 = aug(x2), aug(x2) # aug: random augmentation

        z11, z12 = f(x11), f(x12) # projections
        z21, z22 = f(x21), f(x22) # f: encoder = backbone + projector (mlp)

        p11, p12 = h(z11), h(z12) # predictions
        p21, p22 = h(z21), h(z22) # h: predictor (mlp)

        d1121 = d(z11, z21) # Euclidean distances
        d1122 = d(z11, z22)
        d1221 = d(z12, z21)
        d1222 = d(z12, z22)
        m = min(d1121, d1122, d1221, d1222)

        # D: negative cosine similarity
        # sg: stop-gradient, sg(z) = z.detach()
        if d1121 == m:
            l = D(p11, sg(z12)) + D(p21, sg(z22))
        elif d1122 == m:
            l = D(p11, sg(z12)) + D(p22, sg(z21))
        elif d1221 == m:
            l = D(p12, sg(z11)) + D(p21, sg(z22))
        elif d1222 == m:
            l = D(p12, sg(z11)) + D(p22, sg(z21))
        loss.append(0.5 * l)

    loss = sum(loss) / len(loss) # mean
    loss.backward() # back-propagate
    update(f, h) # SGD update
```

*These authors contributed equally to this work.

B Data augmentation details

B.1 ImageNet

The training set consists of 1,281,167 images, and the validation dataset consists of 50,000 images. Since the label of ImageNet’s test set is not provided, we use the validation set for evaluation. The number of classes in ImageNet is 1,000. The images are variable-sized, so they are cropped to size 224×224 during the data augmentation process. We apply in turn the following data transformations in pre-training.

- **RandomResizedCrop**: Crop a random patch of the image with scale $(0.2, 1)$ and then resize it to a size of $(224, 224)$.
- **ColorJitter**: With a probability of 0.8, change the image’s brightness, contrast, saturation, and hue with strength $(0.4, 0.4, 0.4, 0.1)$.
- **RandomGrayscale**: With a probability of 0.2, convert the image to grayscale.
- **GaussianBlur**: With a probability of 0.5, apply the Gaussian blur filter to the image with a radius uniformly sampled from $[0.1, 2]$.
- **RandomHorizontalFlip**: With a probability of 0.5, flop the image horizontally.
- **Normalize**: Normalize the image with mean $(0.485, 0.456, 0.406)$ and standard deviation $(0.229, 0.224, 0.225)$.

B.2 CIFAR-10

The training set consists of 60,000 images, and the test set consists of 10,000 images. The number of classes in CIFAR-10 is 10. The images have a fixed size of 32×32 . We apply in turn the following data transformations in pre-training.

- **RandomResizedCrop**: Crop a random patch of the image with scale $(0.08, 1)$ and then resize it to a size of $(32, 32)$.
- **RandomHorizontalFlip**: With a probability of 0.5, flop the image horizontally.
- **ColorJitter**: With a probability of 0.8, change the image’s brightness, contrast, saturation, and hue with strength $(0.4, 0.4, 0.4, 0.1)$.
- **RandomGrayscale**: With a probability of 0.2, convert the image to grayscale.
- **Normalize**: Normalize the image with mean $(0.485, 0.456, 0.406)$ and standard deviation $(0.229, 0.224, 0.225)$.

C Pre-training implementation details

C.1 ImageNet

For the ImageNet experiments, we follow the experimental setup in SimSiam’s original paper [Chen and He, 2021] and <https://github.com/facebookresearch/simsiam>. The encoder f consists of a backbone and a projector. The backbone is ResNet-50 [He et al., 2016] with about 23M parameters, and the projector consists of three fully-connected (FC) layers. Batch normalization (BN) and ReLU are applied to each layer except for the output layer, where only BN is used. The input and output dimensions of the layers are 2,048. The predictor h consists of two FC layers. BN and ReLU are applied to the first layer, and nothing is applied to the second layer. The input and output dimensions of the first layer are 2,048 and 512, and the input and output dimensions of the second layer are 512 and 2,048 (bottleneck structure).

C.2 CIFAR-10

For the CIFAR-10 experiments, we follow the default setup in [Susmelj et al., 2020] and <https://github.com/lightly-ai/lightly>. The encoder f consists of a backbone and a projector. The backbone is a variant of ResNet-18 for CIFAR-10 with about 11M parameters, and the projector consists of two FC layers. BN and ReLU are applied to the first layer, and only BN is

applied to the second layer. The input and output dimensions of the first layer are 512 and 2,048, and the input and output dimensions of the second layer are 2,048. The predictor h is the same as in the case of ImageNet.

D Transfer learning implementation details

We present the implementation details for transfer learning. Other details can be found in [Ericsson et al., 2021] and <https://github.com/linusericsson/ssl-transfer>. We minimally change the code under the same computational parameters.

D.1 Image recognition

In the Caltech dataset, 30 images for each class are randomly selected to form the training set, and the remaining images form the test set. On the DTD and SUN397 datasets, the first dataset split provided by the authors is used. For validation sets, the pre-defined ones are used on the Aircraft, DTD, Flowers, and VOC2007 datasets, and on the rest of the datasets, 20% of the training set are randomly selected to form the validation set.

We resize the images so that the number of pixels of the shorter side of each image is 224 using bicubic interpolation. We crop the images at the center with size (224, 224). The best weight decay rate is selected on the validation set over 45 evenly spaced values from 10^{-6} to 10^5 on a logarithmic scale with base 10. We find the best hyperparameters on the validation set, retrain the networks on the training and validation sets, and evaluate on the test set. Since VOC2007 is a multi-label dataset, we fit a binary classifier for each class. L-BFGS [Liu and Nocedal, 1989] is used as a solver when doing a logistic regression.

D.2 Object detection

We initially normalize the images with mean (123.675, 116.280, 103.530) and standard deviation (58.395, 57.120, 57.375).

Pascal-VOC The images are resized so that the number of pixels of the shorter side of each image is one of {480, 512, 544, 576, 608, 640, 672, 704, 736, 768, 800} for training and 800 for test. We use the batch size of 2. The base learning rate is chosen as 0.0025, and it decays by tenths at the 96,000th and 128,000th iterations, respectively. We warm up the networks for 100 iterations and train them for 144,000 iterations.

MS-COCO The images are resized so that the number of pixels of the shorter side of each image is one of {640, 672, 704, 736, 768, 800} for training and 800 for test. We use the batch size of 16. We choose the base learning rate as 0.02, and it decays by tenths at the 210,000th and 250,000th iterations, respectively. We warm up the networks for 1000 iterations and train them for 270,000 iterations.

D.3 Semantic segmentation

We use the SGD optimizer with momentum of 0.9, learning rate of 0.02, weight decay rate of 0.0001, and learning rate decay rate of 0.9. We use the batch size of 2. The networks are trained for 150,000 iterations in total (30 epochs and 5,000 iterations per epoch). The learning rate decays every 500 iterations.

E t-distributed stochastic neighbor embedding (t-SNE)

We present t-SNE visualizations [Van der Maaten and Hinton, 2008] of representations of images from the test set of CIFAR-10. Figure 6 shows that in both SimSiam and BYOL, applying our GSG made the clusters corresponding to the classes better separate.

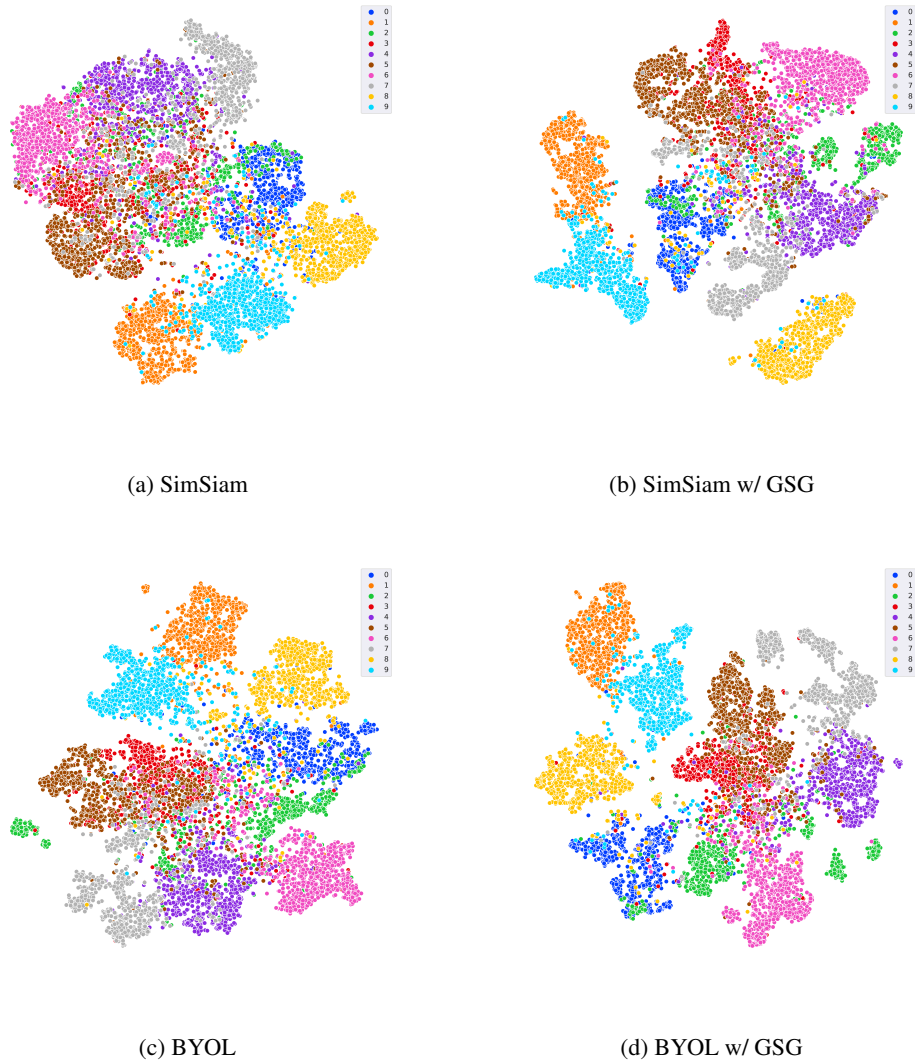


Figure 6: t-SNE visualizations of CIFAR-10. Clusters of our algorithms are better separated than those of the original algorithms as expected.

F Semantic segmentation

We present semantic segmentation results (test image, ground truth, and predicted results of each algorithm) of the first ten images from the validation set of ADE20K. Figure 7 shows that the representations pre-trained by our algorithms transfer well to the semantic segmentation task. Also, the performance of our algorithms is similar to or better than that of the existing algorithms.

G Limitations and future directions

Since this is the first study in the direction of implicitly applying the idea of contrastive learning, we adopt algorithms with simple losses (such as SimSiam and BYOL) as the benchmark algorithms. To do so, we want to see vividly and not to obscure the effect of our method. The performance may be further improved when applied to algorithms that utilize more complicated strategies. For example, there are algorithms that use a multi-crop strategy [Caron et al., 2020] where both global and local views are considered [Caron et al., 2021, Zhang et al., 2022, Wanyan et al., 2023]. Combining our

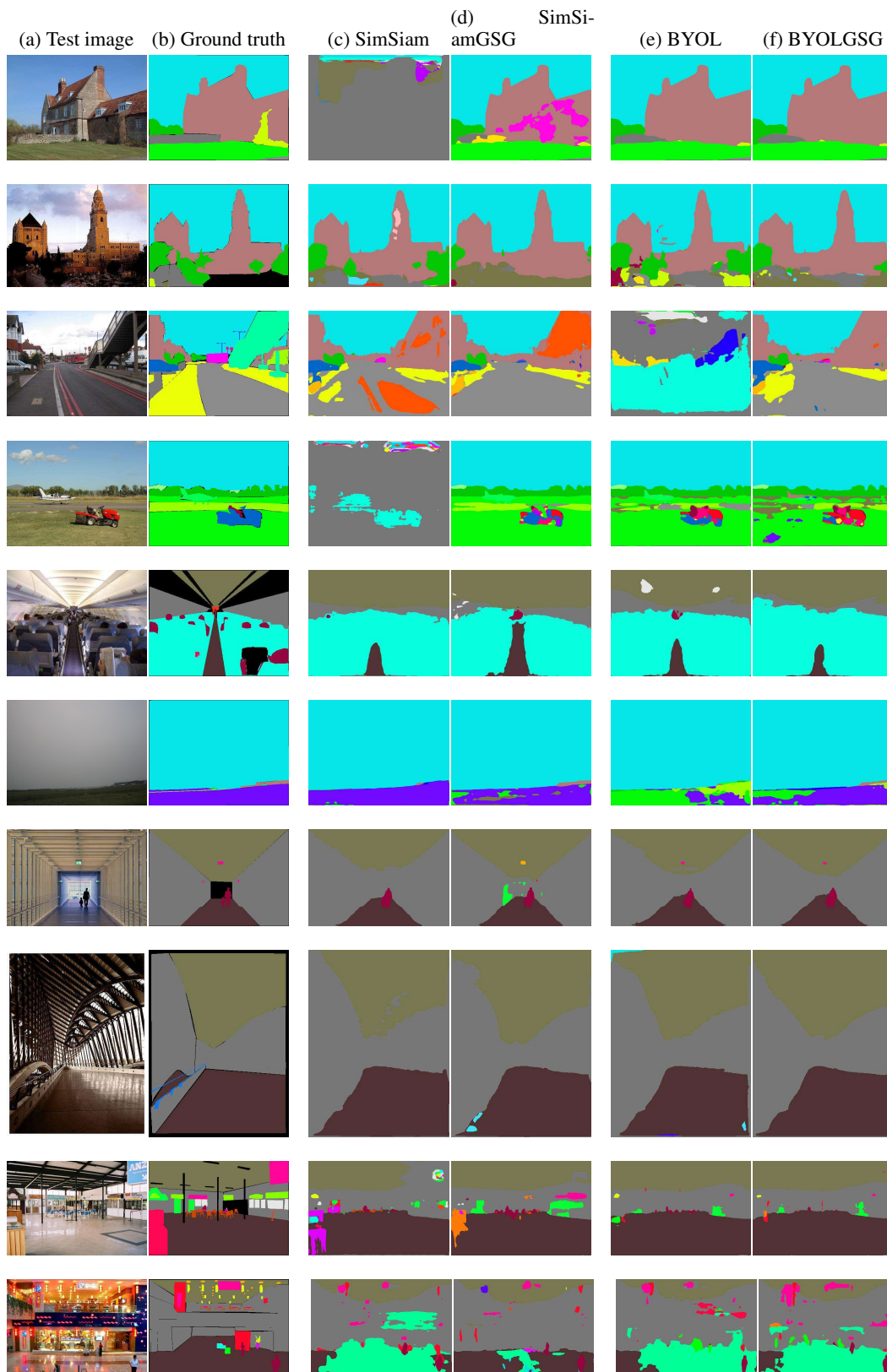


Figure 7: Semantic segmentation results of the first ten images from the validation set of ADE20K. The performance of our algorithms is similar or better than that of the original algorithms.

ideas with these algorithms may further improve transfer learning (e.g., dense prediction tasks) performance on multi-object datasets. Since our methodology is an intermediate between contrastive and non-contrastive learning, it may help the community to better understand the differences and similarities between them [Garrido et al., 2022].

References

- Mathilde Caron, Ishan Misra, Julien Mairal, Priya Goyal, Piotr Bojanowski, and Armand Joulin. Unsupervised learning of visual features by contrasting cluster assignments. *Advances in Neural Information Processing Systems*, 33:9912–9924, 2020.
- Mathilde Caron, Hugo Touvron, Ishan Misra, Hervé Jégou, Julien Mairal, Piotr Bojanowski, and Armand Joulin. Emerging properties in self-supervised vision transformers. In *Proceedings of the IEEE/CVF International Conference on Computer Vision*, pages 9650–9660, 2021.
- Xinlei Chen and Kaiming He. Exploring simple siamese representation learning. In *Proceedings of the IEEE/CVF Conference on Computer Vision and Pattern Recognition*, pages 15750–15758, 2021.
- Linus Ericsson, Henry Gouk, and Timothy M Hospedales. How well do self-supervised models transfer? In *Proceedings of the IEEE/CVF Conference on Computer Vision and Pattern Recognition*, pages 5414–5423, 2021.
- Quentin Garrido, Yubei Chen, Adrien Bardes, Laurent Najman, and Yann Lecun. On the duality between contrastive and non-contrastive self-supervised learning. *arXiv preprint arXiv:2206.02574*, 2022.
- Kaiming He, Xiangyu Zhang, Shaoqing Ren, and Jian Sun. Deep residual learning for image recognition. In *Proceedings of the IEEE conference on computer vision and pattern recognition*, pages 770–778, 2016.
- Dong C Liu and Jorge Nocedal. On the limited memory bfgs method for large scale optimization. *Mathematical programming*, 45(1-3):503–528, 1989.
- Igor Susmelj, Matthias Heller, Philipp Wirth, Jeremy Prescott, and Malte Ebner et al. Lightly. *GitHub*. Note: <https://github.com/lightly-ai/lightly>, 2020.
- Laurens Van der Maaten and Geoffrey Hinton. Visualizing data using t-sne. *Journal of machine learning research*, 9(11), 2008.
- Xinye Wanyan, Sachith Seneviratne, Shuchang Shen, and Michael Kirley. Dino-mc: Self-supervised contrastive learning for remote sensing imagery with multi-sized local crops. *arXiv preprint arXiv:2303.06670*, 2023.
- Tong Zhang, Congpei Qiu, Wei Ke, Sabine Süsstrunk, and Mathieu Salzmann. Leverage your local and global representations: A new self-supervised learning strategy. In *Proceedings of the IEEE/CVF Conference on Computer Vision and Pattern Recognition*, pages 16580–16589, 2022.